Journal of Biogeography (J. Biogeogr.) (2008) **35**, 951–964

ORIGINAL ARTICLE

Relationships between expanding pinyon–juniper cover and topography in the central Great Basin, Nevada

Bethany A. Bradley[1]* and Erica Fleishman[2]

[1]*Woodrow Wilson School, Princeton University, Princeton, NJ, USA,* [2]*National Center for Ecological Analysis and Synthesis, Santa Barbara, CA, USA*

*Correspondence: Bethany A. Bradley, Woodrow Wilson School, Princeton University, Princeton, NJ 08544, USA.
E-mail: bethanyb@princeton.edu

ABSTRACT

Aim Increasing geographical range and density of conifers is a major form of land-cover change in the western United States, affecting fire frequency, biogeochemistry and possibly biodiversity. However, the extent and magnitude of the change are uncertain. This study aimed to quantify the relationship between changing conifer cover and topography.

Location The central Great Basin in the state of Nevada, USA.

Methods We used a series of Landsat Thematic Mapper satellite images from 1986, 1995 and 2005 to map change in pinyon–juniper woodlands (*Pinus monophylla*, *Juniperus* spp.) in the montane central Great Basin of Nevada. We derived fractional greenness for each year using spectral mixture analysis and identified all areas with an above average increase in greenness from 1986 to 1995 and 1995 to 2005.

Results Areas with high fractional greenness in 2005 were most likely to occur at elevations between 2200 and 2600 m a.s.l. Increases in fractional greenness between 1986 and 2005 were most likely to occur at elevations below 2000 m a.s.l. and on south-facing slopes. However, relationships between elevation and increasing greenness for individual mountain ranges varied considerably from the average trend. Fractional greenness values measured by Landsat suggest that the majority of pinyon–juniper woodlands have not reached their maximum potential tree cover.

Main conclusions Expansion of pinyon–juniper at low elevations and on south-facing slopes probably reflects increasing precipitation in the 20th century, higher water use efficiency caused by increasing atmospheric CO_2 in the late 20th century and livestock grazing at the interface between shrubland and woodland. Identification of the spatial relationships between changing fractional greenness of pinyon–juniper woodland and topography can inform regional land management and improve projections of long-term ecosystem change.

Keywords

Conifer expansion, land-cover change, Landsat, Nevada, remote sensing, spatial modelling, spectral mixture analysis, woody encroachment.

INTRODUCTION

Land-cover change is a major component of global change (Foley *et al.*, 2005). Many forms of land-cover change, such as deforestation and urbanization, are directly associated with land use. Other land-cover changes, such as melting of permafrost, may be indirectly associated with human activity via anthropogenically induced climate change. Further changes in land cover, such as the expansion of woody plants, may be caused by a combination of natural climate variability, anthropogenic land use and climate change. Our ability to understand and mitigate the anticipated effects of continued global climate change (Vitousek *et al.*, 1997) will benefit from examining ecosystems in

www.blackwellpublishing.com/jbi
doi:10.1111/j.1365-2699.2007.01847.x

which large-scale land-cover changes are currently being observed.

Across the Intermountain West, marked range expansion of pinyon–juniper woodlands, especially into sagebrush steppe, and increasing density of pinyon and juniper trees has been noted for decades (Burkhardt & Tisdale, 1976; Tausch *et al.*, 1981). Expansion of pinyon–juniper woodlands is believed to have begun in the late 1800s (Miller & Rose, 1995). Several natural and anthropogenic factors have been implicated as potential drivers. First, a 60-year period of relatively warm temperatures and high precipitation in the Great Basin, beginning in the 1880s, may have induced expansion. This hypothesis is consistent with pollen records spanning the Holocene that show substantial shifts in the extent of pinyon and juniper in response to trends in temperature and precipitation (Miller & Wigand, 1994; Gray *et al.*, 2006). Second, intensive and widespread grazing by cattle and sheep transformed the landscape, removing most herbaceous species that might compete with pinyon and juniper for limiting resources (Miller & Rose, 1995). Finally, throughout the 20th century, woodlands were subjected to direct fire suppression as well as indirect suppression via roads, which inhibit the spread of fire, and by sustained livestock grazing that removed fine fuels (Burkhardt & Tisdale, 1976).

Regardless of its causes, pinyon–juniper expansion affects landscape biogeochemistry as well as habitat for and distribution of other species (Archer, 1994; Archer *et al.*, 2001). For example, increasing shade leads to declines in herbaceous cover (Miller *et al.*, 2000) and declines in cover and biomass of sagebrush (subspecies of *Artemisia tridentata*) (Tausch & West, 1995). Woodland expansion also decreases available surface and subsurface water (Huxman *et al.*, 2005).

Conifer expansion has been identified as a major factor in the United States' carbon budget. Increasing tree cover leads to higher above-ground carbon storage (Archer *et al.*, 2001), which has a substantial impact on the carbon budget when the increase is spatially extensive (Houghton *et al.*, 1999; Pacala *et al.*, 2001). However, pinyon–juniper expansion also increases the probability of fire in general and of high-intensity fire in particular, which may negate any gains in carbon storage. Within federal and state land management agencies, fire and fire surrogates, such as thinning or chaining, increasingly are being considered as tools to minimize woodland expansion and the accompanying risk of major wildfires (Ansley & Rasmussen, 2005; National Biological Information Infrastructure, 2007).

Several studies have used remote sensing to map woody plants (Pickup & Chewings, 1994; Hudak & Wessman, 1998; Harris *et al.*, 2003; Afinowicz *et al.*, 2005; McGlynn & Okin, 2006; Powell & Hansen, 2007; Weisberg *et al.*, 2007). These studies focused primarily on land-cover classification or detection of land-cover change using high-resolution aerial photographs or airborne hyperspectral imagery. However, a disadvantage of using aerial photographs and high-resolution imagery, relative to multi-spectral sensors like Landsat Thematic Mapper (TM), is reduced spatial and temporal coverage. Landsat TM has been used successfully to detect changes in forest cover in the north-eastern United States (Sader *et al.*, 2005), and should also be effective in western coniferous forests and woodlands. Assessment of change over large spatial extents with remote sensing requires a method that uses repeat measurements taken with the same sensor and includes data from a sufficiently large area to be considered representative for geospatial modelling.

Two studies have explored the spatial relationship between the distribution of pinyon–juniper woodland and topography using extensive plot data. Tausch *et al.* (1981) recorded tree age and cover across 40 mountain ranges in the Great Basin. They found that tree cover was greatest within intermediate-elevation bands of 2000–2200 m, suggesting climatic control of the distribution of pinyon–juniper woodland. Johnson & Miller (2006) sampled the age and cover of western juniper (*Juniperus occidentalis*) on 186 plots in four watersheds in southern Oregon. They found that establishment of trees was greatest at high elevations and on north-facing slopes. Synthesizing field data with spatially extensive remote sensing data provides the opportunity to improve models of the relationship between conifer expansion and topography.

Weisberg *et al.* (2007) compared aerial photography from 1966 and 1995 to assess change in pinyon–juniper cover in Nevada's Simpson Park Range. They found increases in tree cover of up to 33% within 20-m pixels. Expansion was most extensive at low elevations, although infilling was also observed at higher elevations. Testing the spatial relationships observed in numerous plot-level studies (Tausch *et al.*, 1981; Tausch & Tueller, 1990; Johnson & Miller, 2006) across a broader spatial area is a critical step in the study of any land-cover change and tests the wider applicability of field studies to land management.

In this study we examine relationships between topography, cover of pinyon–juniper woodland and changes in cover of pinyon–juniper woodland across several mountain ranges in the central Great Basin using three Landsat TM images spanning 20 years. Our approach uses the green vegetation component of a linear spectral mixture analysis (SMA) model. The green vegetation component is correlated with the commonly used normalized difference vegetation index (NDVI), but is a slightly better predictor of quantity of photosynthetic vegetation in semi-arid systems (Elmore *et al.*, 2000). Our analysis had three components. First, we quantified fractional greenness (fG) in 2005 and evaluated its relationship to field measurements of tree cover. Second, we identified locations in which fractional greenness had changed over the 20-year period (ΔfG). The goal of this step was not to quantify absolute change in tree cover, but to compile spatially explicit data on locations where any change in cover had occurred. Finally, we conducted a geospatial analysis to assess relationships between current fractional greenness, changes in fractional greenness and topography. The aim of our work is to improve understanding of woodland dynamics in the Intermountain West and to inform land managers' decision-making.

STUDY AREA ECOSYSTEM

Two of the most characteristic trees in the Great Basin of the western United States, often covering the lower to intermediate elevations of mountain slopes, are single-leaf pinyon (*Pinus monophylla*) and juniper (*Juniperus* spp., primarily *Juniperus osteosperma*). Pinyon and juniper frequently grow in mixed stands, although juniper typically begin to grow and cease to occur at slightly lower elevations than pinyon (Grayson, 1993). Trees rarely exceed 6 m in height (Grayson, 1993). In general, pinyon–juniper woodland occurs from 1500 to 2500 m a.s.l. and in areas where mean annual precipitation ranges from 30 to 45 cm (Grayson, 1993). Temperature also affects distributional patterns of both species. Individual trees may live for many hundreds of years. Fire usually kills pinyon and juniper, especially when trees are relatively small and young (Zlatnik, 1999; Zouhar, 2001). Taller or older trees often survive surface fires. The estimated fire interval for pinyon–juniper woodland varies widely across the US Intermountain West as a function of geography, topography and productivity, but typically ranges from 15 to 200 years (Zlatnik, 1999; Zouhar, 2001). However, during the past several centuries, relatively low densities of trees and an absence of fine fuels prevented most fires in pinyon–juniper woodland from becoming severe or continuous.

The study area encompasses the mountain ranges of the central Great Basin captured by Landsat path 41, row 33, including the Desatoya, Shoshone, Toiyabe, Toquima, Monitor and Hot Creek ranges (Fig. 1). Elevations within this area vary from a low of 1300 m a.s.l. in the valleys to a high of 3600 m a.s.l. in the Toiyabe Range. Valleys are characterized by sagebrush steppe, with the more xerophytic species of shrubs (*Atriplex* spp.) at the lowest elevations. Mountain slopes contain woodland communities dominated by pinyon and juniper in a matrix of sagebrush and some perennial bunchgrasses. Within areas of pinyon–juniper woodland are to be found spatially disjunct riparian zones that frequently include deciduous species of trees such as cottonwood, willow or aspen. At the highest elevations, woodland gives way to more mesic shrubland with various perennial bunchgrasses and forbs.

The vast majority of our study area is public land. In general, the valleys are managed by the US Bureau of Land Management and mountain ranges are managed by the US Forest Service. Pinyon–juniper woodlands within the study area are rarely affected by direct anthropogenic land-cover change in the form of clearing or agriculture. However, the study area has been subjected to long-term livestock grazing, primarily of cattle since the mid-1900s, at lower and intermediate elevations.

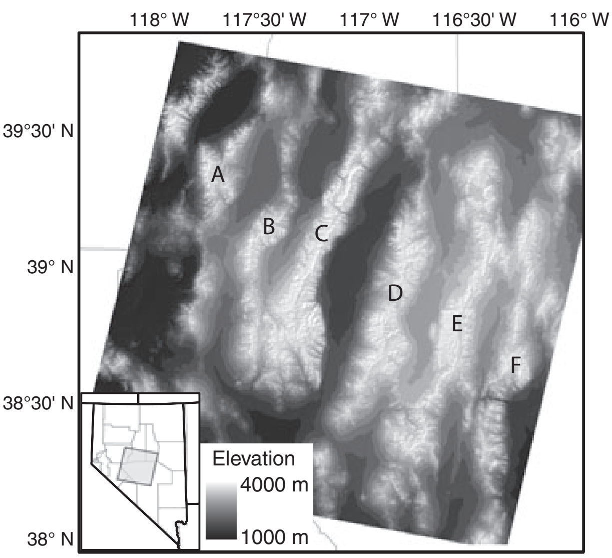

Figure 1 Location of the study area (Landsat TM path 41, row 33) in the central Great Basin, Nevada. Across the region, mountains alternate with valleys. Letters A–F mark the Desatoya, Shoshone, Toiyabe, Toquima, Monitor and Hot Creek ranges, respectively.

METHODS

We acquired Landsat images from mid-October of 1986, 1995 and 2005. At this time of year deciduous trees, grasses and forbs are dormant, but pinyon and juniper are still photosynthetically active. Accordingly, pinyon–juniper woodland is easier to identify and mapped distributions of land-cover change are likely to reflect changes in the tree canopy. We selected these years because they cover a long period of record, thus maximizing detection of change, and because their climatic conditions were similar (Table 1).

Nineteen years is sufficient to expect gradually increasing tree cover to be detectable remotely. Further, because all images were acquired by the same satellite, the analysis is not subject to error associated with differences in spectral or spatial resolution. Late summer conditions during all three years were drier than the long-term average, while minimum and maximum temperatures were close to the long-term average (Table 1). By choosing years that were fairly dry, we reduced the potential effect of phenological variability among years on our results.

Image processing

We co-registered the three images to within 1 pixel (28.5 m). We then georeferenced the images using road intersections apparent in both the images and a US census-based road shapefile. We included a digital elevation model in the georeferencing process to improve accuracy. The final registration accuracy was within 1 pixel both spatially and temporally. Next, we converted the images to reflectance using the radiometric gain and offset values associated with the Landsat TM satellite. We used a dark pixel subtraction to account for atmospheric scatter (Chavez, 1988).

To ensure that reflectance values could be compared directly among years, we radiometrically normalized the 1986 and 1995 images to the 2005 image (Schott *et al.*, 1988). We converted 1986 and 1995 reflectance values to 2005 reflectance using a

Table 1 Average precipitation and temperature (± standard deviation) preceding the dates of measurement for Landsat images included in our analyses. Values are derived from the Parameter-elevation Regressions on Independent Slopes Model (PRISM) (Daly *et al.*, 2002)

Date	10 Oct 1986	3 Oct 1995	14 Oct 2005	30-year average
Total monthly precipitation (mm)				
August	11.6	11.0	10.0	17.1 ± 5.4
September	4.9	4.7	10.6	17.8 ± 4.3
October	11.0	0.4	14.6	18.8 ± 4.9
Average maximum temperature (°C)				
August	30.5	29.5	28.9	29.2 ± 2.3
September	20.5	25.9	22.8	24.4 ± 2.2
October	16.8	19.5	17.7	17.6 ± 2.2
Average minimum temperature (°C)				
August	11.2	9.1	10.6	9.7 ± 1.6
September	3.1	5.9	4.3	5.4 ± 1.5
October	−0.2	−0.8	0.6	0.1 ± 1.3

gain and offset correction. We selected 21 2 × 2 pixel regions from the 2005 image that encompassed a range of pseudo-invariant reflectance values, from dark to bright, for the six visible and near-infrared bands. Reflectance values at these sites in 1986 and 1995 were used to convert the images for those years into 2005 reflectance values. The fits of lines used to spectrally align the images had R^2 values > 0.99 in all cases.

After the Landsat images were geographically and spectrally aligned, we calculated the percentage of green vegetation in each pixel using spectral mixture analysis (SMA) (Smith *et al.*, 1990; Adams *et al.*, 1995; Elmore *et al.*, 2000). This process assumes that every pixel is a linear combination of spectral endmembers, or spectrally homogeneous materials such as soil or green vegetation which are present within a pixel. The result of an unmixing analysis is an estimate of the percentage cover of each of those endmembers for every pixel. Measurements of vegetation change over time have also utilized NDVI. Although use of NDVI would be appropriate in this case, we elected to measure change in the green vegetation component of SMA because it correlates better to percentage cover in semi-arid systems (Elmore *et al.*, 2000).

In this study we used four spectral endmembers: one green pinyon pine leaf (needle) spectrum derived from the US Geological Survey hyperspectral library (Clark *et al.*, 2003), one shadow to account for topographic shading, and two image-derived soils to account for variation in the non-vegetated ground surface. We did not use a non-photosynthetic (woody) endmember because doing so increased the root mean square error of the overall fit and decreased the correlation between satellite and ground measurements. We used the same four endmembers to perform the spectral unmixing analysis on all three images.

The pinyon pine needle endmember (Clark *et al.*, 2003) was considerably brighter than any image-derived pinyon–juniper pixel. This resulted in underestimates of green vegetation and overestimates of shadow and dark soil. However, use of an image endmember as the green vegetation endmember was less desirable because soils were extremely heterogeneous and maximum tree cover was 65%. Despite the underestimated green vegetation component, this approach provided the best correlation with field measurements of tree cover.

Only the green vegetation component (i.e. fractional green cover as measured by the satellite) was retained for each image. Henceforth, we refer to the fractional green vegetation component as *f*G. We used *f*G values to estimate the proportion of tree cover in 2005 and to identify changes in tree cover (Δ*f*G) between 1986 and 2005.

Field measurements

We compared *f*G to field measurements of pinyon–juniper cover to determine the proportion of field-derived variance explained by the satellite measurements. We measured tree cover using two perpendicular 30-m line transects that intersected at the midpoint. The GPS location of each centre point was recorded. Measurements of tree cover were collected from a total of 33 pairs of transects.

We selected transect locations that were readily accessible by roads or trails and encompassed a range of *f*G values. In addition, spatial variance of *f*G amongst Landsat pixels that surrounded our transects was low. Low spatial variance was desirable because a slight misregistration (< 1 pixel) between ground and satellite could create a large error in a location with highly variable tree cover. We placed transects in the eastern Shoshone, western Toiyabe and eastern Monitor ranges. Field validation was conducted in July 2006. We assumed that tree cover did not change substantially between October 2005 and July 2006.

At each 1-m interval along the field transects, we recorded the 'satellite view' of canopy cover – our best estimate of cover as observed from above the canopy. We differentiated among soil, photosynthetic tree, non-photosynthetic tree (i.e. woody material), photosynthetic shrub, non-photosynthetic shrub and herbaceous cover. Photosynthetic and non-photosynthetic tree values were later pooled to estimate total cover of conifers at the transect location due to the difficulty of distinguishing woody and green tree components from below.

To compare satellite and field measurements, we calculated *f*G values as the mean of all pixels intersecting a circle with 30-m radius extending from the transect centre point. Using a search radius longer than the transect accounted for any possible registration errors. The relationship between Landsat pixel values and validation points demonstrates what derived *f*G values actually represent on the ground.

Identification of 2005 fractional greenness and change in fractional greenness

We restricted our analysis to areas classified as pinyon–juniper in the Southwest ReGAP land-cover classification (US Geological Survey, 2004). We added a buffer of 500 m to the pinyon–juniper woodland extents to include adjacent mixed vegetation that might contain a low proportion of pinyon–juniper cover. In addition to masking areas not classified as pinyon–juniper, we masked out clouds, cloud shadows and agricultural fields. Clouds appeared mainly in the 1986 image, and were digitized and masked by hand. Agricultural fields were identified based on their high *f*G values and circular or rectilinear shapes. In addition, we masked all areas with $f\text{G} \leq 0$ in 2005. We assumed that these pixels did not contain pinyon or juniper and that no change within these pixels was associated with an increase in tree cover.

Areas with high *f*G are important to identify because the probability of fire may increase in areas with high tree cover. We defined high *f*G as the highest 10% (90th percentile) of all Landsat-derived *f*G values, which corresponded to values > 0.14 in 2005. In addition to defining high *f*G, we separated *f*G values into percentiles (10th, 10–25th, 25–75th and 75–90th in addition to 90th) to investigate how total tree cover was related to topography.

To identify areas with changing fractional greenness (Δ*f*G), we first calculated the median Δ*f*G from 1986–95 and from 1995–2005 for all pinyon–juniper pixels. Pixels with Δ*f*G greater than the median in both time periods were considered to have positive Δ*f*G. Pixels with Δ*f*G lower than the median in both time periods were considered to have negative Δ*f*G. We did not establish a more restrictive Δ*f*G threshold (e.g. values greater than the 95th percentile in both time periods) because we wanted to identify all areas of change rather than areas with maximum change.

Due to the flexible threshold for detecting change, a positive or negative Δ*f*G does not necessarily reflect an increase or decrease in greenness. The median Δ*f*G between years may be negative if, for example, productivity during the first year was particularly high. Hence, a local negative Δ*f*G value could actually correspond to an increase in *f*G if the median for the study region is lower than the local value. Similarly, a local positive Δ*f*G value could correspond to a decrease in *f*G if the median Δ*f*G value for the study region is greater than the local value. By using a flexible threshold between increasing and decreasing *f*G based on the population median (i.e. the median of all pixels) rather than a fixed value (e.g. 0, where all positive or negative values indicate change), we reduced the influence of inter-annual variability in tree canopy and understorey greenness on our identification of change.

Based on the change analysis, we identified three categories: areas where fractional greenness had increased (positive Δ*f*G), areas where fractional greenness had decreased (negative Δ*f*G) and areas where no change occurred. We calculated the average *f*G for each year (1986, 1995 and 2005) for pixels with positive Δ*f*G, negative Δ*f*G and no change in order to compare their relative greenness trends.

Topographic relationships

We examined the relationships between topographic variables and the spatial distribution of pixels with high *f*G in 2005. We also examined the relationships between topographic variables and changing *f*G (Δ*f*G). Methods followed Bradley & Mustard (2006). We measured the probability of occurrence of high *f*G in 2005 within discrete ranges of elevation and occurrence of Δ*f*G (classified as change present or change absent for each pixel) within discrete ranges of elevation and aspect. Elevation and aspect were derived from National Elevation Dataset 30-m resolution digital elevation models (National Elevation Dataset, 1999).

Elevation was categorized to approximately equalize the land area within each category rather than equalizing the vertical height of each elevation class. Within each category of elevation or aspect (e.g. elevations 2110–2160 m a.s.l., north-facing slopes), the probability of occurrence of high *f*G in 2005 was calculated as the number of pixels with high *f*G in 2005 divided by the total number of pixels in that category. The same calculation was performed for occurrences of positive Δ*f*G and negative Δ*f*G. All relationships are presented in terms of absolute probability on a scale of 0–1.

We do not report statistical significance for any of the topographic relationships. Remotely sensed results provide a tremendous number of data points, in this case more than 12 million. As a result, all relationships are statistically significant and any error bars are negligible.

RESULTS

Fractional greenness in 2005

Although Landsat-derived values of fractional greenness (*f*G) were much lower than field measurements due to the spectral endmembers utilized, *f*G in 2005 derived from Landsat had a positive relationship with tree cover as measured in the field ($R^2 = 0.56$) (Fig. 2).

We observed high *f*G values throughout pinyon–juniper woodlands, particularly at higher elevations (Fig. 3). The *f*G values tended to increase as elevation increased. Low *f*G values were more common at lower elevations at the transition between sagebrush steppe and pinyon–juniper woodland (Fig. 4). The highest 10% of Landsat-derived *f*G values were most likely to occur at elevations above 2200 m a.s.l., especially between 2400 and 2600 m a.s.l. (Fig. 5). Between 2400 and 2600 m a.s.l., the probability of occurrence of high *f*G values was 0.20. High *f*G values were unlikely to occur below 2000 m a.s.l., and were less likely to occur above 2600 m a.s.l. than at intermediate elevations.

Changing greenness

A total of 3.0 million pinyon–juniper pixels (*c.* 250,000 ha) had Δ*f*G greater than the median in both the 1986–95 and 1995–2005 time periods. Thus, an estimated 25% of pixels had a positive Δ*f*G trend. A total of 1.4 million pinyon–juniper pixels (*c.* 110,000 ha) had Δ*f*G below the median in both 1986–95 and 1995–2005 time periods. Thus, an estimated 11% of pixels had a negative Δ*f*G trend. The direction of change in Δ*f*G for the remaining 7.8 million pixels (*c.* 520,000 ha) was

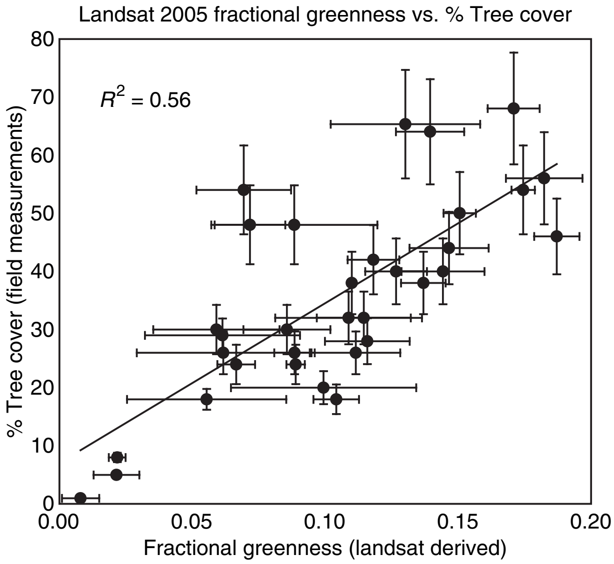

Figure 2 Relationship between 2005 Landsat-derived greenness and 2006 tree cover as measured at 33 pairs of transects in the Shoshone, Toiyabe and Monitor ranges. X error bars are standard deviations of all pixels within 30 m of the centre point of the transect. Y error bars are standard errors of tree cover measured along the line transects.

inconsistent among time periods; these pixels were classified as no change. Relative to the average of pixels with no change, pixels with a positive Δ*f*G trend had a much greater positive slope in *f*G over time (Fig. 6). Similarly, pixels with negative Δ*f*G had a large negative slope over time (Fig. 6). These patterns are expected based on the chosen classification scheme and are shown for illustrative purposes. Average fractional greenness for the study area was higher in 1995 than in either 1986 or 2005.

Areas with positive Δ*f*G were distributed throughout the mountain ranges (Fig. 7). Positive Δ*f*G values were apparent at both high and low elevations, including areas adjacent to sagebrush steppe. Patches of positive Δ*f*G occurred both as large, contiguous areas and as small, scattered areas and single pixels.

Topographic patterns of changing greenness

Between 1986 and 2005, changes in fractional greenness (Δ*f*G) were most likely to be positive at elevations < 2000 m a.s.l. (Fig. 8a). The probability of positive Δ*f*G was 0.30 at elevations below 1760 m a.s.l. (0.05 higher than the average). The probability of positive Δ*f*G from 2000–2600 m a.s.l. was equal to the average (0.25). Above 2600 m a.s.l., the probability of occurrence of positive Δ*f*G fell to 0.15. Conversely, the probability of occurrence of negative Δ*f*G was lowest at low elevations and greatest at high elevations.

The relationship between positive Δ*f*G and elevation differed among mountain ranges (Fig. 8b–d). In the Desatoya Range, the occurrence of positive Δ*f*G was highly probable (as much as 0.42) and the occurrence of negative Δ*f*G was highly improbable, at elevations below 2010 m a.s.l. The occurrence of negative Δ*f*G in the Desatoya Range was most likely at elevations between 2070 and 2330 m a.s.l.

Across the Shoshone Mountains, the probability of occurrence of positive Δ*f*G was 0.35, much higher than in any other mountain range (Fig. 8c). We did not find a high probability of occurrence of either positive or negative Δ*f*G at the lowest elevations in the Shoshone Mountains. However, the lowest elevations in the Shoshone Mountains are higher than in neighbouring mountain ranges. The probability of occurrence of positive Δ*f*G was lowest at elevations > 2530 m a.s.l., while the probability of occurrence of negative Δ*f*G was highest above 2530 m a.s.l.

In the Toiyabe Range, the probability of occurrence of positive Δ*f*G was greatest at elevations below 2010 m a.s.l. (Fig. 8d). The probability of occurrence of positive Δ*f*G was 0.44 at elevations below 1870 m a.s.l. (nearly double the average probability for any pixel in the study area). The probability of occurrence of negative Δ*f*G was low (0.05) at elevations below 2010 m (less than half the probability for any pixel in the study area).

Relationships between aspect and Δ*f*G also were strong (Fig. 9). Relative to all pixels in the analysis, the probability of occurrence of positive Δ*f*G was greatest, and the probability of occurrence of negative Δ*f*G was lowest, on south-facing slopes (112.5–247.5°). Similarly, the probability of occurrence of positive Δ*f*G was lowest, and the probability of occurrence of negative Δ*f*G was greatest, on north-facing slopes (292.5–67.5°). There was little variation in the relationship between aspect and Δ*f*G among mountain ranges.

The effects of elevation and aspect on the probability of occurrence of positive Δ*f*G appeared to be interactive (Fig. 10). Similar to the total population, the probability of occurrence of positive Δ*f*G was greatest on south-facing slopes at low elevations. However, the probability of occurrence of positive Δ*f*G did not increase at low elevations on north-facing slopes.

DISCUSSION

Data on the spatial and temporal pattern of vegetation cover are important for understanding ecosystem processes. The 30-m resolution of Landsat provides spatially extensive information about intermediate-resolution mosaics of land cover. The patterns of these mosaics can inform models of associated ecosystem properties, including the level of solar energy available in open areas, water uptake by woody plants and carbon storage in trees and soils (Breshears, 2006). Relationships between topography and high or increasing greenness may indicate how regional climate influences the expansion and cover of pinyon–juniper woodland.

Information on tree cover also informs land management. Currently, the US Forest Service and other federal agencies use fire and mechanical treatments to minimize expansion of pinyon–juniper woodland and canopy closure (Ansley & Rasmussen, 2005) and associated risks to human habitation

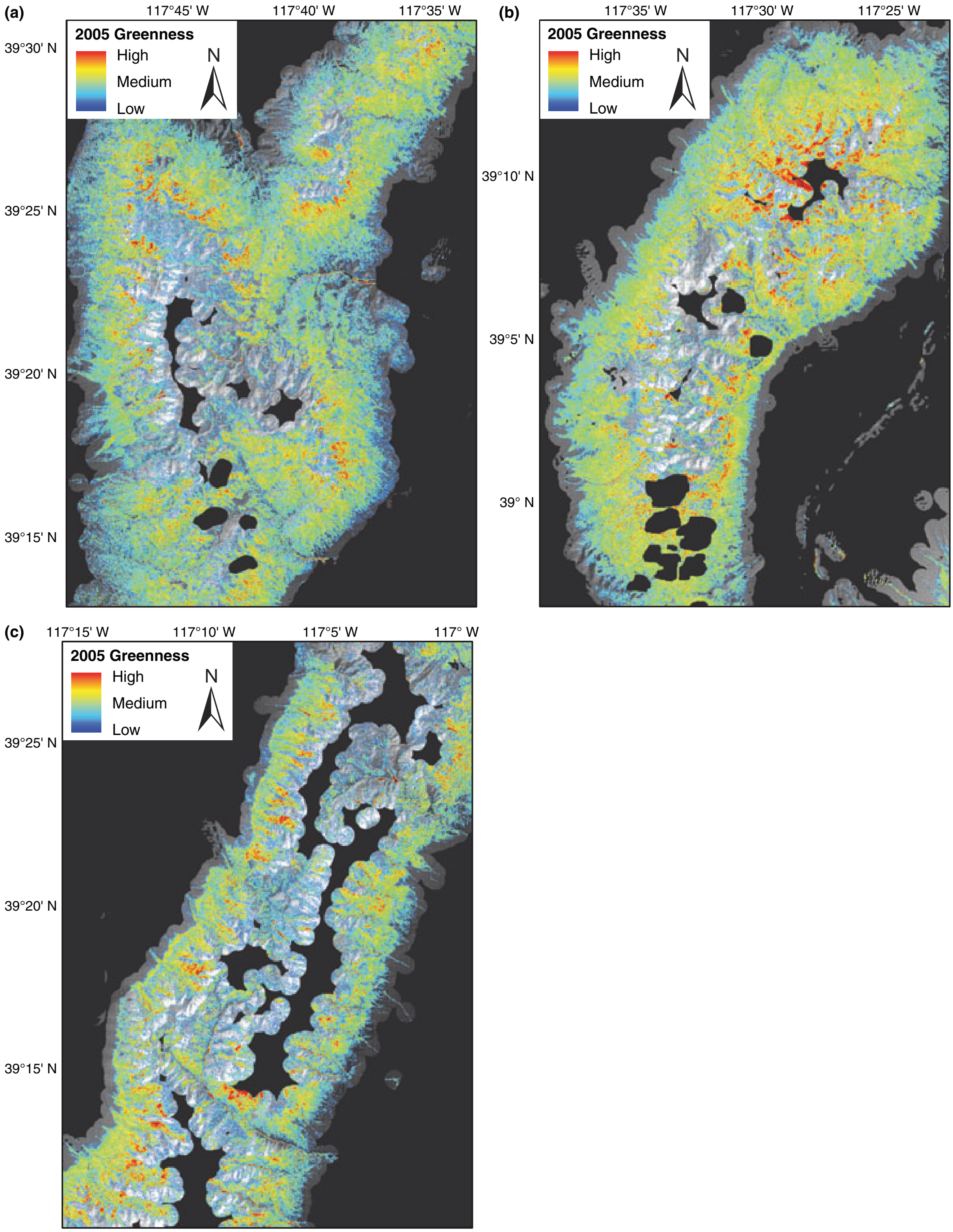

Figure 3 Fractional greenness (*f*G) in October 2005 from Landsat TM. Percentage greenness values were derived from the green vegetation component of a linear spectral unmixing model. Higher *f*G values indicate a higher percentage cover of trees. Dark grey areas have been excluded because they do not represent pinyon–juniper woodland or contain clouds. The background is grey-scale topography over shaded relief. The images shown here encompass portions of the (a) Desatoya Range, (b) Shoshone Mountains and (c) Toiyabe Range.

and desired land uses. Continuous models of crown cover for the Intermountain West are available at a spatial resolution of 250 m (Miles *et al.*, 2001). However, estimates of changes in land cover are only available at discrete point locations (e.g. US Forest Service forest inventory and analysis data). Spectral unmixing of Landsat TM provides spatially explicit estimates

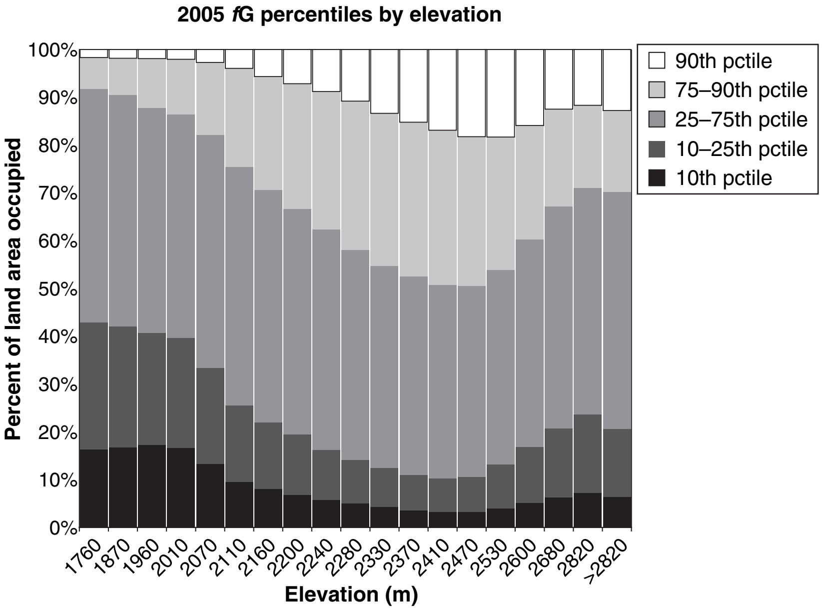

Figure 4 Relationship between 2005 fractional greenness (*f*G) and topography. *f*G values in the 10th percentile (low *f*G) were most likely to occur at elevations below 2110 m. *f*G values in the 90th percentile (high *f*G) were most likely at elevations between 2240 and 2600 m.

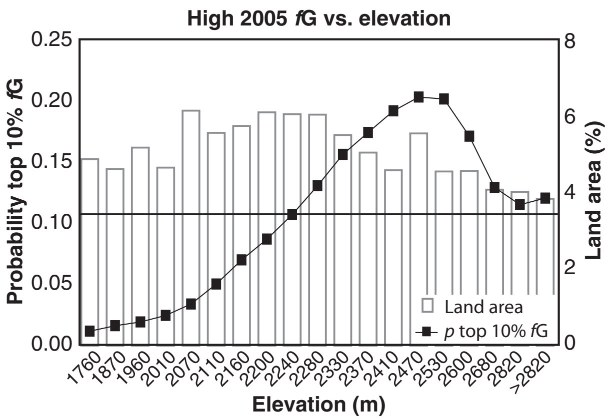

Figure 5 Relationships between elevation and high 2005 fractional greenness (*f*G) (90th percentile) as measured by Landsat. The horizontal line indicates the probability that the *f*G of a given pixel is within the 90th percentile. Bars represent the percentage of land area present within that aspect or elevation threshold.

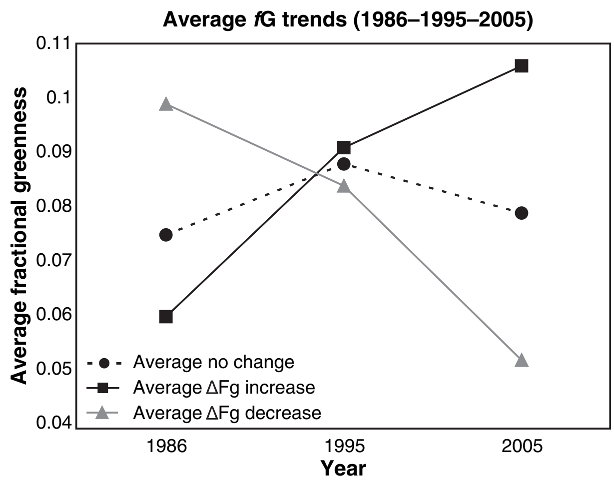

Figure 6 Average fractional greenness (*f*G) values for all Landsat pixels with positive Δ*f*G (above median values for both 1986–95 and 1995–2005), negative Δ*f*G (below median values for both 1986–95 and 1995–2005), and all remaining pixels (no directional change). *f*G values for each year were derived from a linear unmixing model.

of tree cover and changes in tree cover at 30-m resolution that are relevant to adaptive management.

In our work, fractional greenness (*f*G) values derived from remote sensing were positively correlated with tree cover measured in the field. Some of the scatter in the points may be due to undersampling of tree cover in the field (i.e. extrapolating from line transects to polygons or continuous areas). Differences in plot-level greenness can also result from differences in leaf area index (LAI) within the tree canopy. Remotely sensed data are sensitive to the total fraction of green cover, whether the cover results from tree cover or LAI (Carlson & Ripley, 1997). Slight offsets in spatial registration also affect accuracy, as does imprecision in the spectral mixture analysis (SMA) model. The SMA model is further influenced by variation in soil spectral characteristics and understorey cover of woody shrubs, as well as the relative proportions of photosynthetic and non-photosynthetic components within the tree canopy related to LAI.

However, despite the scatter, we found a clear relationship between tree cover and Landsat-derived *f*G that we believe is useful both for ecosystem modelling and for land management. Further, it is likely that positive Δ*f*G observed over the 20-year period is related to change in tree cover because expansion of pinyon–juniper woodland has been observed throughout the Great Basin during this time period (Tausch *et al.*, 1993; Miller & Rose, 1995, 1999; Weisberg *et al.*, 2007).

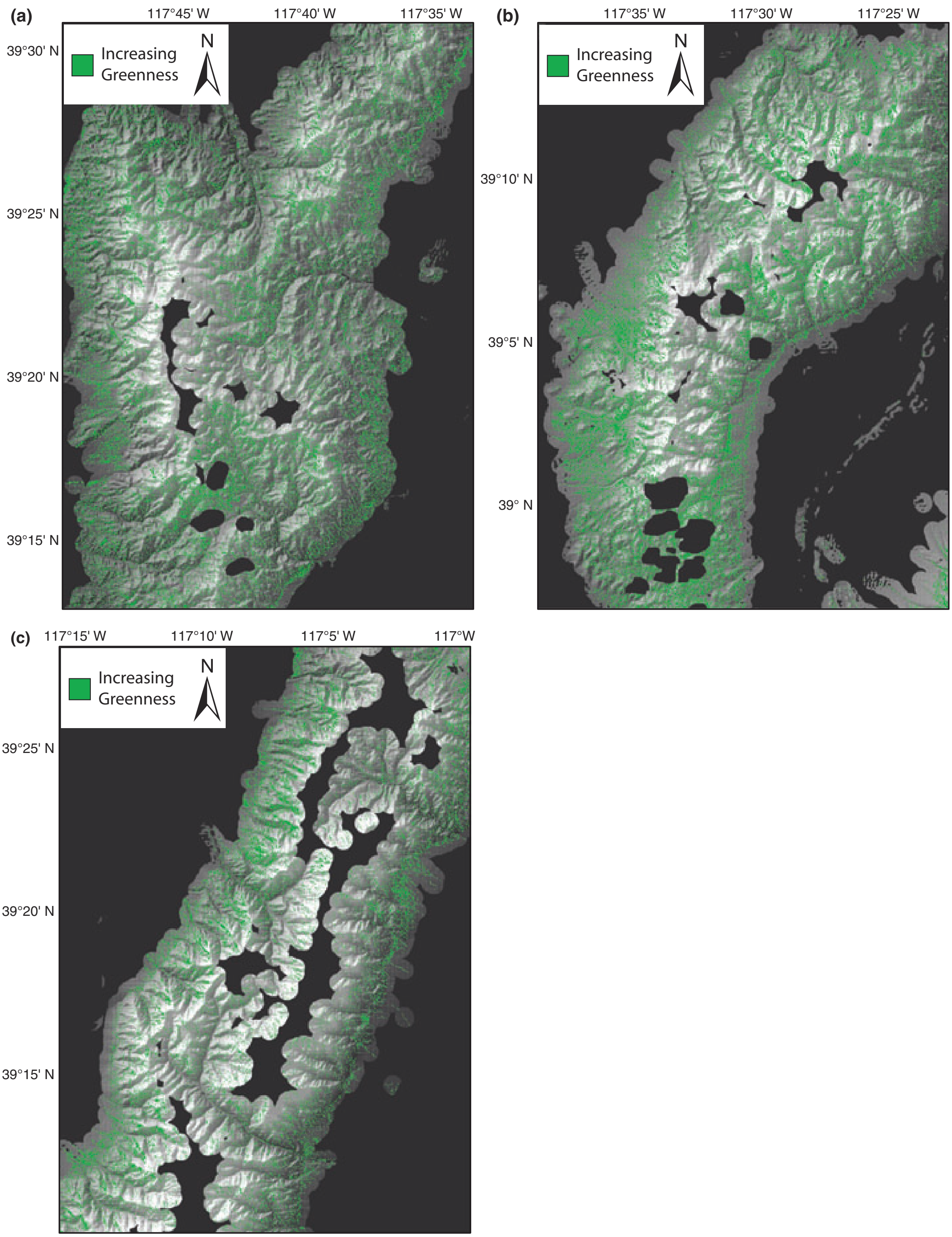

Figure 7 Increasing fractional greenness from 1986–2005. Green areas had positive Δ*f*G values (above median values for both 1986–95 and 1995–2005). Dark grey areas have been excluded because they do not represent pinyon–juniper woodland or contain clouds. The background is grey-scale topography over shaded relief. The images shown here encompass portions of the (a) Desatoya Range, (b) Shoshone Mountains and (c) Toiyabe Range.

Spatial distributions of 2005 fractional greenness

Elevation, which was associated strongly with *f*G in 2005, directly influences temperature and moisture availability. Lower elevations generally are warmer and receive less precipitation than higher elevations.

Across the mountain ranges we sampled, the probability of occurrence of relatively high *f*G values in 2005 was greatest

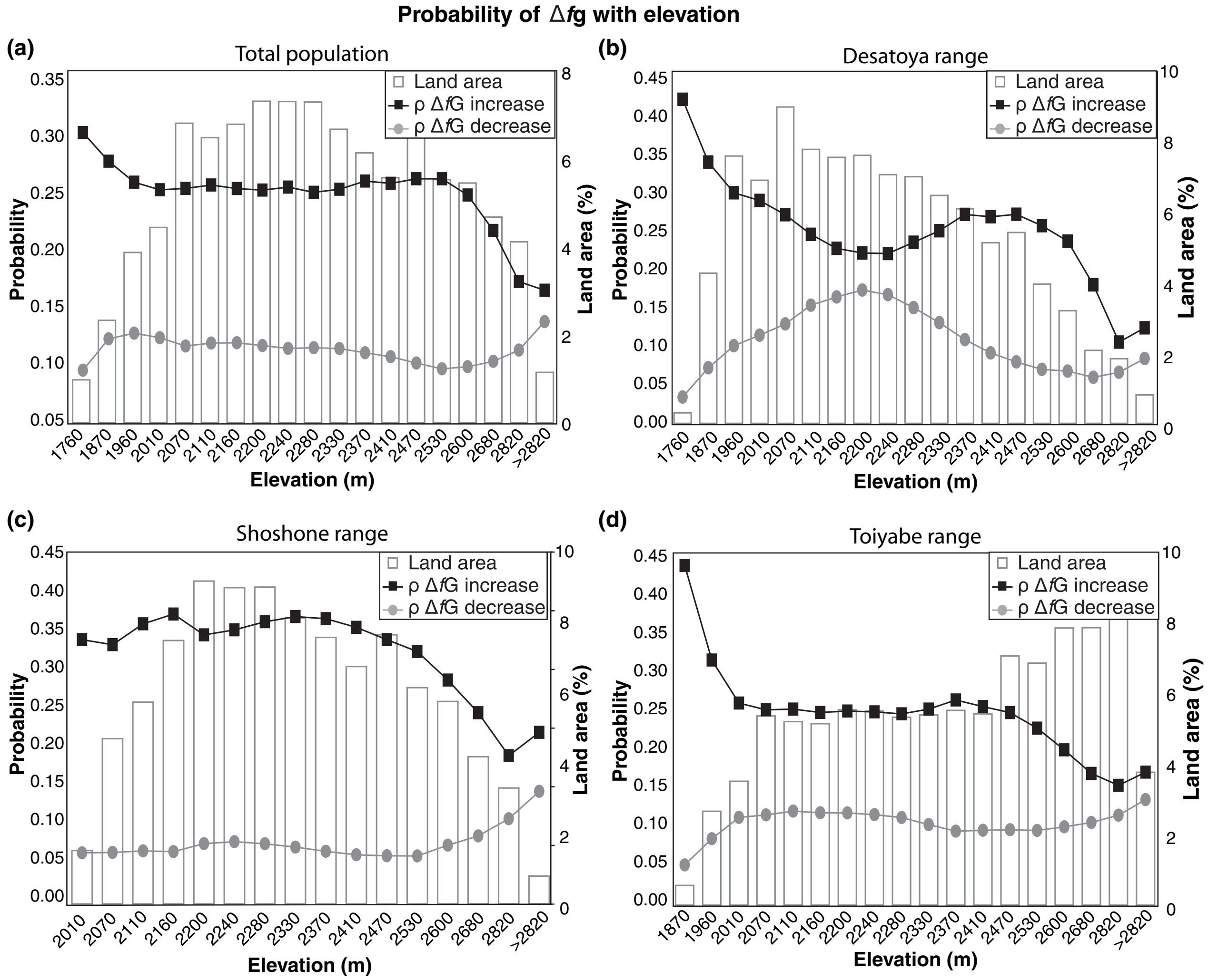

Figure 8 Probability of positive Δ*f*G and negative Δ*f*G in pinyon–juniper woodland at different elevations. Black squares indicate the probability of positive Δ*f*G within each elevation band. Grey circles indicate the probability of negative Δ*f*G within each elevation band. Bars indicate the proportion of land area within each elevation band. The different plots show patterns for (a) the study area, (b) Desatoya Range, (c) Shoshone Mountains and (d) Toiyabe Range.

at elevations from 2300–2600 m a.s.l. (Fig. 5). By comparison, Tausch *et al.* (1981) found that dominance of trees, a measure of tree recruitment in the understorey related to tree density, was greatest from 2000–2200 m a.s.l. across 18 mountain ranges in Nevada and Utah (including the ranges in this study). However, Tausch *et al.* (1981) noted substantial spatial heterogeneity in tree dominance patterns among mountain ranges. The difference in the relationship between *f*G and elevation in our work and the relationship between tree dominance and elevation measured by Tausch *et al.* (1981) may result from differences in measurement criteria. Lower elevations (2000–2200 m a.s.l.) may have high tree density, whereas higher elevations (2300–2600 m a.s.l.) may have lower density but higher tree cover. It is also possible that tree density or tree cover have increased at higher elevations since the observations of Tausch *et al.* (1981).

Increasing tree cover

Detection of changes in tree cover during recent decades is important for understanding the causes of woodland expansion and predicting its cascading ecological effects. Remote sensing data greatly enhance our ability to analyse spatial patterns of woodland expansion (Powell & Hansen, 2007; Weisberg *et al.*, 2007). Pinyon–juniper expansion beginning in the late 1800s was coincident with a slightly wetter climate, the introduction of livestock grazing, increasing atmospheric CO_2 and reduced fire frequency (Burkhardt & Tisdale, 1976; Miller & Wigand, 1994; Miller & Rose, 1995). However, the relative contributions of these changes (or their interactions) to increases in tree cover are uncertain.

Changes in tree cover measured by Landsat can also be used to estimate associated changes in ecosystem processes. Woodland expansion has been linked to changes in soil (Jackson

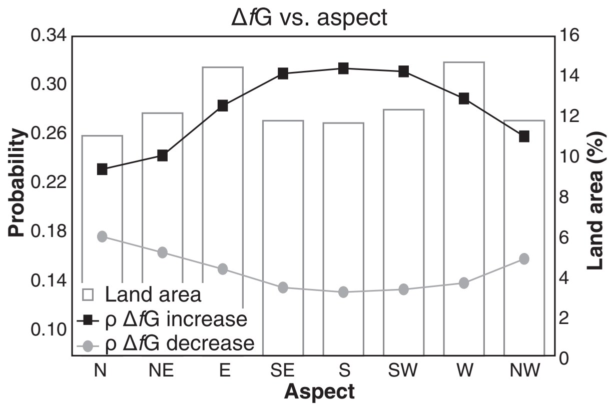

Figure 9 Probability of change in fractional greenness (Δ*f*G) in pinyon–juniper woodlands at different aspects. Black squares indicate the probability of positive Δ*f*G. Grey circles indicate the probability of negative Δ*f*G. Bars indicate the proportion of land area within each aspect class.

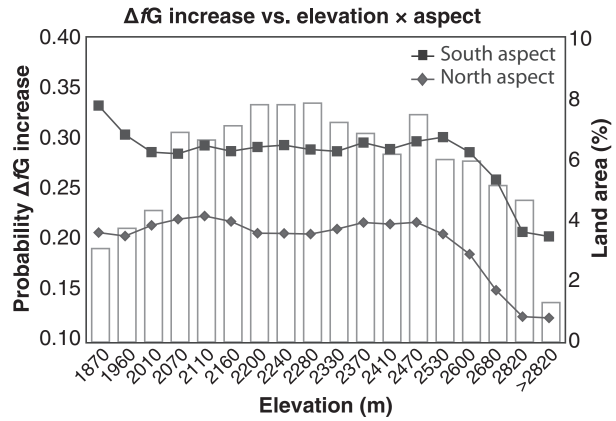

Figure 10 Probability of positive Δ*f*G in pinyon–juniper woodlands at different elevations on north-facing and south-facing slopes. Bars are the proportion of land area present within that aspect or elevation threshold. Black squares indicate the probability of positive Δ*f*G on south-facing slopes. Grey diamonds indicate the probability of positive Δ*f*G on north-facing slopes.

et al., 2002) and aboveground (Archer *et al.*, 2001) carbon storage, and may create a net carbon sink in the United States (Houghton *et al.*, 1999; Pacala *et al.*, 2001). In addition, expansion of pinyon–juniper woodlands impedes the recruitment of shrubs and herbaceous species (Miller *et al.*, 2000).

Because our Landsat images were spatially and spectrally aligned with a high degree of accuracy, and because the same spectral endmembers were used to unmix all three images, we have high confidence in our identification of Δ*f*G. Landsat-derived *f*G for any given year may not precisely match tree cover as measured in the field, but Δ*f*G should represent changes in greenness observed on the ground. In other words, we expect comparisons of relative greenness between years to be more accurate and precise than measures of absolute greenness in any given year.

Spatial distributions of increasing tree cover

Our results indicate that positive Δ*f*G has occurred primarily at low elevations and rarely at high elevations (Fig. 8). These results support previous field observations of expansion of pinyon–juniper woodland (Burkhardt & Tisdale, 1976) as well as recent analyses of change based on aerial photographs (Weisberg *et al.*, 2007). Both climate and land use could favour expansion at low elevations. Slightly higher average precipitation during the 20th century (Miller & Wigand, 1994; Gray *et al.*, 2006) may have facilitated tree recruitment into lower elevations that were previously too dry to support pinyon–juniper woodland. Land use may also favour pinyon–juniper expansion at lower elevations. For example, localized timber harvest for fuel and charcoal in the 19th century may have been concentrated at lower elevations (Reno, 1994), creating conditions for regrowth in the late 20th century. Additionally, livestock grazing at the interface between shrubland and woodland reduces competition from herbaceous species and may promote woodland expansion.

Positive Δ*f*G was more likely on south-facing slopes than on north-facing slopes across the full elevational gradient (Figs 9 & 10). It is likely that tree recruitment on south-facing slopes was enhanced by a longer growing season and greater exposure to sunlight. Relatively high precipitation during the first half of the 20th century may also have increased water availability and tree recruitment on south-facing slopes.

Increased concentrations of atmospheric CO_2 beginning in the late 20th century may also have supported the expansion of pinyon and juniper at low elevations and on south-facing slopes. Elevated CO_2 increases the efficiency of water use by plants by reducing transpiration rates (Farquhar, 1997). Elevated CO_2 levels during the 21st century may allow woodland expansion to continue even if precipitation decreases.

It seems unlikely that changes in temperature were associated with pinyon–juniper expansion into low elevations and south-facing slopes. Temperatures during the 20th century remained constant or increased, a change more likely to cause expansion of woodlands at high elevations and on north-facing slopes than the opposite pattern observed here. Hence, the explanatory factors most consistent with expansion of pinyon and juniper into low elevations and south-facing slopes are increases in precipitation during the 20th century, elevated CO_2 in the late 20th and early 21st centuries, and livestock grazing at the interface between shrubland and woodland.

Although positive Δ*f*G was more likely to occur at low elevations and on south-facing slopes, positive Δ*f*G occurred across the elevational gradient, suggesting that pinyon–juniper woodlands have been expanding throughout the central Great Basin. If this trend continues, crown cover is likely to increase throughout these woodlands, thereby increasing the overall risk of major fires.

Relationships between woodland cover and topography were inconsistent among mountain ranges. Differences in geology, hydrology and topography among ranges are likely to result in different patterns of pinyon–juniper expansion. We emphasize that local variability can strongly influence regional-scale trends. This phenomenon further supports the use of spatially extensive remotely sensed observations in landscape ecology.

CONCLUSION

Cover of pinyon–juniper woodland is increasing throughout the Great Basin and Intermountain West, USA. This form of land-cover change can be identified effectively using remote sensing techniques. Spatial relationships derived from Landsat images can be used for targeted land management and iterative planning and implementation. Our analyses suggest that in the central Great Basin, cover of pinyon–juniper woodland is currently greatest at relatively high elevations (2200–2700 m a.s.l.). However, tree cover has been increasing disproportionately at low elevations, and on south-facing slopes at all elevations. Fractional greenness values measured by Landsat suggest that the majority of pinyon–juniper woodlands have not reached their maximum potential tree cover. Furthermore, livestock grazing at lower elevations and elevated CO_2 acting to increase water use efficiency in drier areas are likely to induce further changes in this system. As a result, continued pinyon–juniper expansion is likely.

ACKNOWLEDGEMENTS

We thank Stephanie Bradley for field assistance and Jeanne Chambers, Robin Tausch, David Dobkin, Rick Miller and two anonymous referees for constructive feedback on the manuscript. Support for this research was provided by the Joint Fire Science Program via the Rocky Mountain Research Station, Forest Service, US Department of Agriculture, the High Meadows Funds (BAB), and the National Fish and Wildlife Foundation.

REFERENCES

Adams, J.B., Sabol, D.E., Kapos, V., Almeida, R., Roberts, D.A., Smith, M.O. & Gillespie, A.R. (1995) Classification of multispectral images based on fractions of endmembers application to land-cover change in the Brazilian Amazon. *Remote Sensing of Environment*, **52,** 137–154.

Afinowicz, J.D., Munster, C.L., Wilcox, B.P. & Lacey, R.E. (2005) A process for assessing wooded plant cover by remote sensing. *Rangeland Ecology & Management*, **58,** 184–190.

Ansley, R.J. & Rasmussen, G.A. (2005) Managing native invasive juniper species using fire. *Weed Technology*, **19,** 517–522.

Archer, S. (1994) Woody plant encroachment into southwestern grasslands and savannas: Rates, patterns and proximate causes. *Ecological implications of livestock herbivory in the west* (ed. by M. Vavra, W. Laycock and R. Pieper), pp. 13–68. Society for Range Management, Denver.

Archer, S., Boutton, T.W. & Hibbard, K.A. (2001) Trees in grasslands: biogeochemical consequences of woody plant expansion. *Global biogeochemical cycles in the climate system* (ed. by D. Schulze, M. Heimann, S. Harrison, E. Holland, J. Lloyd, I. Prentice and D. Schimel), pp. 115–138. Academic Press, San Diego.

Bradley, B.A. & Mustard, J.F. (2006) Characterizing the landscape dynamics of an invasive plant and risk of invasion using remote sensing. *Ecological Applications*, **16,** 1132–1147.

Breshears, D.D. (2006) The grassland–forest continuum: trends in ecosystem properties for woody plant mosaics? *Frontiers in Ecology and the Environment*, **4,** 96–104.

Burkhardt, J.W. & Tisdale, E.W. (1976) Causes of juniper invasion in southwestern Idaho. *Ecology*, **57,** 472–484.

Carlson, T.N. & Ripley, D.A. (1997) On the relation between NDVI, fractional vegetation cover, and leaf area index. *Remote Sensing of Environment*, **62,** 241–252.

Chavez, P.S. (1988) An improved dark-object subtraction technique for atmospheric scattering correction of multispectral data. *Remote Sensing of Environment*, **24,** 459–479.

Clark, R.N., Swayze, G.A., Wise, R., Livo, K.E., Hoefen, T.M., Kokaly, R.F. & Sutley, S.J. (2003) *USGS digital spectral library splib05a*. US Geological Survey Open File Report 03-395. US Geological Survey, Denver.

Daly, C., Gibson, W.P., Taylor, G.H., Johnson, G.L. & Pateris, P. (2002) A knowledge-based approach to the statistical mapping of climate. *Climate Research*, **22,** 99–113.

Elmore, A.J., Mustard, J.F., Manning, S.J. & Lobell, D.B. (2000) Quantifying vegetation change in semiarid environments: Precision and accuracy of spectral mixture analysis and the normalized difference vegetation index. *Remote Sensing of Environment*, **73,** 87–102.

Farquhar, G.D. (1997) Carbon dioxide and vegetation. *Science*, **278,** 1411.

Foley, J.A., Defries, R., Asner, G.P., Barford, C., Bonan, G., Carpenter, S.R., Chapin, F.S., Coe, M.T., Daily, G.C., Gibbs, H.K., Helkowski, J.H., Holloway, T., Howard, E.A., Kucharik, C.J., Monfreda, C., Patz, J.A., Prentice, I.C., Ramankutty, N. & Snyder, P.K. (2005) Global consequences of land use. *Science*, **309,** 570–574.

Gray, S.T., Betancourt, J.L., Jackson, S.T. & Eddy, R.G. (2006) Role of multidecadal climate variability in a range extension of pinyon pine. *Ecology*, **87,** 1124–1130.

Grayson, D.K. (1993) *The desert's past: a natural prehistory of the Great Basin*. Smithsonian Institution Press, Washington.

Harris, A.T., Asner, G.P. & Miller, M.E. (2003) Changes in vegetation structure after long-term grazing in pinyon-juniper ecosystems: integrating imaging spectroscopy and field studies. *Ecosystems*, **6,** 368–383.

Houghton, R.A., Hackler, J.L. & Lawrence, K.T. (1999) The U.S. carbon budget: contributions from land-use change. *Science*, **285,** 574–578.

Hudak, A.T. & Wessman, C.A. (1998) Textural analysis of historical aerial photography to characterize woody plant encroachment in South African savanna. *Remote Sensing of Environment*, **66,** 317–330.

Huxman, T.E., Wilcox, B.P., Breshears, D.D., Scott, R.L., Snyder, K.A., Small, E.E., Hultine, K., Pockman, W.T. & Jackson, R.B. (2005) Ecohydrological implications of woody plant encroachment. *Ecology*, **86,** 308–319.

Jackson, R.B., Banner, J.L., Jobbagy, E.G., Pockman, W.T. & Wall, D.H. (2002) Ecosystem carbon loss with woody plant invasion of grasslands. *Nature*, **418,** 623–626.

Johnson, D.D. & Miller, R.F. (2006) Structure and development of expanding western juniper woodlands as influenced by two topographic variables. *Forest Ecology and Management*, **229,** 7–15.

McGlynn, I.O. & Okin, G.S. (2006) Characterization of shrub distribution using high spatial resolution remote sensing: ecosystem implications for a former Chihuahuan Desert grassland. *Remote Sensing of Environment*, **101,** 554–566.

Miles, P.D., Brand, G.J., Alreich, C.L., Bednar, L.F., Woudenberg, S.W., Glover, J.F. & Ezzell, E.N. (2001) *The forest inventory and analysis database: database description and users manual*, *version 1.0*. General Technical Report NC-218, p. 130. US Department of Agriculture, Forest Service, North Central Research Station, St Paul.

Miller, R.F. & Rose, J.A. (1995) Historic expansion of *Juniperus occidentalis* (western juniper) in southeastern Oregon. *Great Basin Naturalist*, **55,** 37–45.

Miller, R.F. & Rose, J.A. (1999) Fire history and western juniper encroachment in sagebrush steppe. *Journal of Range Management*, **52,** 550–559.

Miller, R.F. & Wigand, P.E. (1994) Holocene changes in semiarid pinyon-juniper woodlands. *BioScience*, **44,** 465–474.

Miller, R.F., Svejcar, T.J. & Rose, J.A. (2000) Impacts of western juniper on plant community composition and structure. *Journal of Range Management*, **53,** 574–585.

National Biological Information Infrastructure (2007) *Fire research and management exchange system: fire and fire surrogates study*. http://frames.NBII.gov (accessed January 2007).

National Elevation Dataset (1999) *USGS 30 meter resolution national elevation dataset (NED)*. US Geological Survey, Sioux Falls.

Pacala, S.W., Hurtt, G.C., Baker, D., Peylin, P., Houghton, R.A., Birdsey, R.A., Heath, L., Sundquist, E.T., Stallard, R.F., Ciais, P., Moorcroft, P., Caspersen, J.P., Shevliakova, E., Moore, B., Kohlmaier, G., Holland, E., Gloor, M., Harmon, M.E., Fan, S.M., Sarmiento, J.L., Goodale, C.L., Schimel, D. & Field, C.B. (2001) Consistent land- and atmosphere-based U.S. carbon sink estimates. *Science*, **292,** 2316–2320.

Pickup, G. & Chewings, V.H. (1994) A grazing gradient approach to land degradation assessment in arid areas from remotely-sensed data. *International Journal of Remote Sensing*, **15,** 597–617.

Powell, S.L. & Hansen, A.J. (2007) Conifer cover increase in the Greater Yellowstone ecosystem: frequency, rates, and spatial variation. *Ecosystems*, **10,** 204–216.

Reno, R.L. (1994) *The charcoal industry in the Roberts Mountains, Eureka county, Nevada*. ARS Report No. 600; BLM Report No. CRR-06-1193(P). Bureau of Land Management, Virginia City, NV.

Sader, S., Hoppus, M., Metzler, J. & Jin, S. (2005) Perspectives of Maine forest cover change from Landsat imagery and Forest Inventory Analysis (FIA). *Journal of Forestry*, **103,** 299–303.

Schott, J.R., Salvaggio, C. & Volchok, W.J. (1988) Radiometric scene normalization using pseudoinvariant features. *Remote Sensing of Environment*, **26,** 1–14.

Smith, M.O., Ustin, S.L., Adams, J.B. & Gillespie, A.R. (1990) Vegetation in deserts. 1. A regional measure of abundance from multispectral images. *Remote Sensing of Environment*, **31,** 1–26.

Tausch, R.J. & Tueller, P.T. (1990) Foliage biomass and cover relationships between tree-dominated and shrub-dominated communities in pinyon–juniper woodlands. *Great Basin Naturalist*, **50,** 121–134.

Tausch, R.J. & West, N.E. (1995) Plant species composition patterns with differences in tree dominance on a southwestern Utah pinyon–juniper site. *Proceedings of the desired future conditions for pinyon–juniper ecosystems*, US Forest Service General Technical Report RM-258 (ed. by D.W. Shaw, E.F. Aldon and C. Losapio), pp. 16–23. USDA Forest Service Rocky Mountain Forest and Range Experiment Station, Fort Collins, CO.

Tausch, R.J., West, N.E. & Nabi, A.A. (1981) Tree age and dominance patterns in Great-Basin pinyon-juniper woodlands. *Journal of Range Management*, **34,** 259–264.

Tausch, R.J., Wigand, P.E. & Burkhardt, J.W. (1993) Viewpoint – plant community thresholds, multiple steady-states, and multiple successional pathways – legacy of the Quaternary. *Journal of Range Management*, **46,** 439–447.

US Geological Survey (2004) *National gap analysis program. Southwest regional gap analysis project field sample database*. RS/GIS Laboratory, College of Natural Resources, Utah State University, Logan, UT.

Vitousek, P.M., Mooney, H.A., Lubchenco, J. & Melillo, J.M. (1997) Human domination of Earth's ecosystems. *Science*, **277,** 494–499.

Weisberg, P.J., Lingua, E. & Pillai, R.B. (2007) Spatial patterns of pinyon–juniper woodland expansion in central Nevada. *Rangeland Ecology and Management*, **60,** 115–124.

Zlatnik, E. (1999) *Juniperus osteosperma. Fire Effects Information System [online]*. US Department of Agriculture, Forest Service, Rocky Mountain Research Station, Fire Sciences Laboratory. http://www.fs.fed.us/database/feis/ (accessed August, 2007).

Zouhar, K.L. (2001) *Pinus monophylla. Fire Effects Information System [online]*. US Department of Agriculture, Forest Service, Rocky Mountain Research Station, Fire Sciences Laboratory. http://www.fs.fed.us/database/feis/ (accessed August, 2007).

BIOSKETCHES

Bethany Bradley is a post-doctoral research associate in the Woodrow Wilson School at Princeton University. She received a PhD in Geological Sciences from Brown University. She is interested in the applications of remote sensing and spatial analysis to understanding change in terrestrial ecosystems.

Erica Fleishman is the director of ecosystem-based management programs at the National Center for Ecological Analysis and Synthesis. She received a PhD in Ecology, Evolution and Conservation Biology from the University of Nevada, Reno. She is interested in the spatial distributions of species and how distributions are influenced by land use and management decisions.

Editor: David Bowman